Biophysical Chemistry 40 (1991) 89–96
Elsevier Science Publishers B.V., Amsterdam

BIOCHE 01557

Enzyme-inhibitor complexes of lysozyme with glucosamine inhibitors

A molecular dynamics study through ^{2}H-NMR

László Szilágyi * and Péter Forgó

Department of Organic Chemistry, L. Kossuth University, Pf. 20, H-4010 Debrecen, Hungary

Received 27 July 1990
Revised manuscript received 19 October 1990
Accepted 7 November 1990

NMR, ^{2}H-; Lysozyme; Molecular dynamics; *N*-Acetyl-D-glucosamine; Enzyme-inhibitor complex

^{2}H relaxation measurements coupled with multiple specific ^{2}H labeling have provided insight into the molecular dynamics of *N*-acetyl-D-glucosamine (GlcNAc) inhibitors bound to lysozyme. Deuteron T_1 and T_2 data for the bound state of methyl α- and -β-GlcNAc ^{2}H-labeled in the glycosidic methyl and C2 positions have been derived from measurements at different enzyme/inhibitor ratios. Rotational correlation times calculated therefrom for the labeled sites indicate, in both cases, tight binding for the sugar ring ($\tau_b = 3.0 \times 10^{-9}$ s) accompanied by fast internal rotation, about one axis, of the glycosidic methyl groups ($\tau_r = 5.5\text{–}7.6 \times 10^{-11}$ s). The small but consistent difference in the rates of internal rotation for the α- and β-anomeric inhibitors may be indicative of different solution structures of the enzyme-inhibitor complexes.

1. Introduction

Studies of enzyme-inhibitor interactions can provide valuable information towards understanding enzyme activity. Hen egg white lysozyme represents one of the most scrutinized systems [1]. Studies of its complexes with *N*-acetyl-D-glucosamine (GlcNAc), GlcNAcβ(1 → 4)GlcNAc and GlcNAcβ(1 → 4)GlcNAcβ(1 → 4)GlcNAc by X-ray crystallography and supplemented by model building have been instrumental in an early proposal for the mechanism of lysozyme catalysis [2,3]. Since most enzyme-catalyzed reactions take place in solution, it is of prime interest to gain insight into solution structures and dynamics of small molecules interacting with enzymes. Among the factors contributing to the spectacular rate enhancements by enzymes immobilization of the substrate on the binding site certainly plays an important role. In this respect, one of the most intriguing questions concerns the manner in which the motional characteristics of the small molecule (inhibitor, substrate, co-enzyme, allosteric effector, etc.) change upon binding.

Such processes can be best studied by NMR relaxation measurements, since nuclear relaxation is a function of rotational correlation times characteristic of molecular motions. The ^{2}H nucleus (deuteron) is especially attractive for such purposes for several reasons. First, unlike non-quadrupolar nuclei (^{1}H, ^{13}C, etc.), ^{2}H relaxation is completely dominated by a single mechanism: the quadrupolar interaction. In contrast, multiple contributions such as dipolar, chemical shift anisotropy or spin rotation can complicate the relaxation behavior of spin-1/2 nuclei, such as ^{1}H, ^{13}C, ^{31}P, etc. Second, quadrupolar relaxation is, in all circumstances, intramolecular in origin. This,

* To whom correspondence should be addressed.

0301-4622/91/$03.50

again, is not the case with spin-1/2 nuclei whose dipolar relaxation, for instance, can have both intra- and intermolecular contributions. Third, it is relatively facile to introduce the deuterium label in high isotopic purity into specific locations of a molecule to provide thereby sensitive probes that report motions at the labeled sites. Last, but not least, labeled molecules enable measurements to be performed with any degree of selectivity required, at reasonably low concentrations compatible with enzyme systems, and without background perturbations from signals of the non-labeled components (non-labeled sites of the small molecule or the enzyme).

We have previously investigated [4] the molecular dynamics of binding to lysozyme of methyl α- and β-*N*-acetyl-D-glucosaminide inhibitors labeled by ^{2}H at the *N*-acetylmethyl group. A similar study has subsequently been reported [5] on wheat germ agglutinin.

In order to gain more insight into the details of molecular motions of bound inhibitors, multiple selective ^{2}H labeling is required. To this end, we have synthesised methyl α- and β-*N*-acetyl-D-glucosaminides labeled with ^{2}H at the glycosidic methyl groups and at the C-2 site of the tetrahydropyrane sugar ring and performed molecular dynamics studies of lysozyme binding through ^{2}H-relaxation measurements.

2. Methods

The observed spin-lattice, and spin-spin relaxation rates for a small molecule (I) exchanging between a 'free' and a 'bound' (EI) environment in a simple equilibrium,

$$\mathrm{E} + \mathrm{I} \underset{k_4}{\overset{k_3}{\rightleftharpoons}} \mathrm{EI}, \tag{1}$$

are given [6,7] as:

$$\frac{1}{T_{i\mathrm{obs}}} = \frac{1}{T_{if}} + C\frac{1}{T_{i\mathrm{M}}} = \frac{1}{T_{if}} + C\frac{1}{T_{i\mathrm{b}} + \tau_{\mathrm{M}}} \tag{2}$$

$(i = 1, 2)$

where T_{if} and $T_{i\mathrm{b}}$ denote the relaxation times in the free and bound states, respectively, $\tau_{\mathrm{M}} = k_4^{-1}$ is the lifetime of molecule I in the EI complex and $C = [\mathrm{EI}]/[\mathrm{I}_0]$ is the mole fraction of molecules I bound to E. The apparent relaxation time for the bound inhibitor, $T_{i\mathrm{M}}$, is directly obtained from fitting the experimental data ($T_{i_{\mathrm{obs}}}$, C) to eq. 2. It contains the exchange contribution, τ_{M}, which is to be determined independently to allow evaluation of $T_{i\mathrm{b}}$. Eq. 2 is valid for $T_{if} \gg T_{i\mathrm{b}}$, $C \ll 1$ and it is furthermore assumed that the chemical shift difference between the free and bound state is negligible.

The quantity of interest is $T_{i\mathrm{b}}$, the relaxation time of the nucleus observed in the bound state of I. For quadrupolar relaxation specifically [8],

$$\frac{1}{T_{i\mathrm{b}}} = \frac{3}{8}\left(\frac{e^2qQ}{\hbar}\right)^2 \cdot f_i(\tau_{\mathrm{b}});\ i = 1, 2 \tag{3}$$

where e^2qQ/h is the quadrupolar coupling constant and τ_{b} the correlation time for the motion of the relaxation vector (in our case the C–^{2}H bond) in the bound state. $(T_{i\mathrm{b}})^{-1}$, in general, is also a function of the Larmor frequency, ω, of the nucleus observed,

$$\frac{1}{T_{1\mathrm{b}}} = \frac{3}{40}\left(\frac{e^2qQ}{\hbar}\right)^2 \cdot [J(\omega) + 4J(2\omega)]$$

$$= \frac{3}{8}\left(\frac{e^2qQ}{\hbar}\right)^2 \cdot f_1(\tau_{\mathrm{b}}, \omega), \tag{4}$$

$$\frac{1}{T_{2\mathrm{b}}} = \frac{3}{40}\left(\frac{e^2qQ}{\hbar}\right)^2 \cdot [1.5J(0) + 2.5J(\omega) + J(2\omega)]$$

$$= \frac{3}{8}\left(\frac{e^2qQ}{\hbar}\right)^2 \cdot f_2(\tau_{\mathrm{b}}, \omega). \tag{5}$$

The particular forms of the spectral density functions, $J(n\omega)$, depend on the details of the motion of the relaxation vector. Two models will be distinguished here.

(a) Isotropic overall tumbling with no internal rotation present. In this case the spectral densities are functions of a single correlation time (τ_{b}) only. Then

$$J(0) = \tau_{\mathrm{b}};\ J(\omega) = \frac{\tau_{\mathrm{b}}}{1 + (\omega\tau_{\mathrm{b}})^2};$$

$$J(2\omega) = \frac{\tau_{\mathrm{b}}}{1 + (2\omega\tau_{\mathrm{b}})^2} \tag{6}$$

(b) Isotropic overall reorientation with internal rotation around one rotation axis. Two correlation times are associated with this model: τ_c for the overall rotation and τ_r for the internal rotation. When the latter is described by a rotational diffusion process, the following spectral densities are obtained [9,10]:

$$J(0) = \tau_c$$

$$J(n\omega) = \tfrac{1}{4}(3\cos^2\theta - 1)^2 \frac{\tau_c}{1 + (n\omega\tau_c)^2} + \tfrac{3}{4}\sin^4\theta \frac{\tau_1}{1 + (n\omega\tau_1)^2} + 3\sin^2\theta\cos^2\theta \frac{\tau_2}{1 + (n\omega\tau_2)^2}$$

$$\text{with } n = 1, 2; \frac{1}{\tau_1} = \frac{1}{\tau_c} + \frac{2}{3\tau_r}; \frac{1}{\tau_2} = \frac{1}{\tau_c} + \frac{1}{6\tau_r} \quad (7)$$

and θ being the angle between the relaxation vector and the internal rotation axis. When the internal rotation is fast compared with the overall tumbling rate ($\tau_r \ll \tau_c$) and τ_r is within the extreme narrowing limit the relaxation rates in the bound state, as calculated [10] for the quadrupolar mechanism, are:

$$\frac{1}{T_{ib}} = 9.51 \times 10^9 \cdot [f_i(\tau_c) + 120\tau_r], \; i = 1, 2 \quad (8)$$

with

$$f_1(\tau_c) = \frac{\tau_c}{1 + (\omega\tau_c)^2} + \frac{4\tau_c}{1 + (2\omega\tau_c)^2} \quad (8a)$$

$$f_2(\tau_c) = 1.5\tau_c + \frac{2.5\tau_c}{1 + (\omega\tau_c)^2} + \frac{\tau_c}{1 + (2\omega\tau_c)^2} \quad (8b)$$

if θ is taken to be equal to the tetrahedral angle (109° 28′) and $e^2qQ/h = 170$ kHz.

3. Experimental

Specifically ^{2}H-labeled methyl *N*-acetyl α- and β-D-glucosaminide inhibitors **1a**, **1a′** and **1b**, **1b′**, respectively, have been prepared according to published procedures [20,21]. The ^{2}H content was approx. 90% for **1a′** and **1b′** and approx. 98% for **1a** and **1b**. Because of partial overlap, in the ^{2}H-NMR spectrum, of OC^2H_3 and C2-^{2}H resonances, ^{2}H relaxation measurements were carried out separately on isotopomers **1a** and **1a′** (or **1b** and **1b′**), respectively.

Lysozyme (3 × crystallized) was obtained from Sigma and used without further purification. All measurements were carried out at pH 6.0 in 0.066 M phosphate buffer made up with deuterium-depleted water. The fraction of the inhibitor bound to lysozyme (C) was varied from 0 to approx. 0.07 starting from the largest value and then diluting the sample with an inhibitor stock solution so that the inhibitor concentration remained constant throughout a particular run. The sample temperature was maintained at 35 ± 1°C using a Bruker B-VT 1000 temperature control unit. Association constants, $K = [EI]/[E][I]$, were taken from ref. 13. The complexed fraction, $C = [EI]/[I_0]$, of the inhibitor is then calculated [4] as *

$$C = \left[K[E_0] + K[I_0] + 1 - \sqrt{(K[E_0] + K[I_0] + 1)^2 - 4[E_0][I_0]K^2}\right] \times [2[I_0]K]^{-1} \quad (9)$$

with $[E_0]$ and $[I_0]$ being the analytical concentrations of lysozyme and inhibitor, respectively. Enzyme concentrations have been determined from the ultraviolet absorption at 280 nm with $\epsilon_M = 3.6 \times 10^4$ M^{-1} cm^{-1} [22].

^{2}H-NMR measurements at 30.72 MHz were carried out on a Bruker WP 200 SY in the unlocked mode using 10 mm outer diameter sample tubes. The field homogeneity was carefully adjusted, especially for linewidth determinations, in the locked mode, using a sample of deuterium oxide. The lineshape was found to be reasonably close to Lorentzian as judged by the line-fitting routine (FP-J) or the Bruker DISNMR software, $\Delta\nu_{1/2}$ being 1.4–1.8 Hz for different runs of non-spinning samples. The same shim settings were then applied for all subsequent runs and special care was taken to maintain the sample volume and

* This formula is reproduced here in the correct form because of printing errors in our previous paper [4].

position in the probe head unchanged during a measurements session. The linewidth of the residual HDO signal in the phosphate buffer was approx. 4.5 Hz under the same conditions and did not change appreciably in samples containing different amounts of lysozyme. The width and lineshape of this signal have therefore served to monitor the field homogeneity during all measurements. ^{2}H $\Delta\nu_{1/2}$ values have been obtained by deconvolution of the spectra into component peaks through a SIMPLEX iterative fitting procedure [14] using Lorentzian lineshapes. A typical fit is shown in fig. 3.

^{2}H (30.72 MHz) and ^{13}C (50.32 MHz) T_1 determinations have been performed by the inversion-recovery method employing a quadratically arrayed set [23] of 9–13 variable τ values and a GROPE-16 [24] 180° pulse. The 90° pulse width was 16 μs (10-mm samples) and 9.5 μs (5-mm samples) for ^{2}H and ^{13}C, respectively. A waiting time of at least $5T_1$ has been inserted between successive scans and 300–800 scans have been accumulated for each delay setting in the case of ^{2}H measurements. Calculation of the T_1 values was performed by three-parameter iterative fitting of the T_1 routine of Bruker's DISNMRP package. Typical standard deviation of the fitting was approx. 5%.

4. Results and discussion

The molecular dynamics of the free inhibitors have been inferred from ^{2}H and ^{13}C relaxation measurements. The ^{13}C-NMR spectra have been determined for samples unenriched in ^{13}C and ^{2}H and the ^{13}C assignments were taken from ref. 25. Relevant data are summarized in table 5. It is seen that essentially identical rotational correlation times are obtained from the ^{13}C and ^{2}H relaxation data if the quadrupolar coupling constant for the C-^{2}H bond is taken equal to 170 kHz. It has been shown [4,10,11] that this value is reasonable for a saturated C–^{2}H bond.

The effective rotational correlation times for the *O*-methyl groups are about an order of magnitude smaller than those for the ^{2}H label at position 2, characteristic of the overall motion of the sugar ring. This is due to the internal rotation of the methyl groups. It has been shown [5,9] that in case of multiple fast internal rotations ($\tau_c \geqslant 10\tau_r$) around more than one axis, each one contributes a factor of $1/4[(3\cos^2\theta - 1)^2]$ to the effective correlation time, wherein θ is the angle from internal rotation axis (n) to ($n-1$), or to the label axis of interest, for the last rotation. For $\theta \approx 109°$ (tetrahedral angle) the above factor is roughly 0.1. It is clear therefore that fast internal rotation for the *O*-methyl groups can occur around only one axis in both anomeric inhibitors (**1a** and **1b**, for instance) although two rotations are conceivable (C1⟩O and O⟩CD$_3$). Intramolecular hydrogen bonding and/or an exo-anomeric effect [12] may explain this observation.

For the inhibitors in the bound state (EI), the apparent relaxation times, T_{iM}, are readily calculated from a linear fit of the observed relaxation rates to eq. 2. The experimental $T_1(^2\text{H})$ data for the glycosidic *O*-trideuteromethyl groups in **1a** and **1b** as determined in the presence of various amounts of lysozyme are summarized in tables 1 and 2 and a linear fit is shown in fig. 1. To obtain T_{ib}, the quantity of interest, the exchange contribution, τ_M, must be known. τ_M is equal to the reciprocal of the dissociation rate constant, k_4, in

Table 1

$T_1(^2\text{H})$ values measured for methyl-d$_3$ *N*-acetyl-α-D-glucosaminide (**1a**) in the presence of increasing amounts of lysozyme [a]

$C = [\text{EI}]/[\text{I}_0]$ [b]	T_1(OMe) (s)
0.00	0.453
9.66×10^{-4}	0.452
2.28×10^{-3}	0.439
2.59×10^{-3}	0.432
6.12×10^{-3}	0.417
7.75×10^{-3}	0.405
1.01×10^{-2}	0.394
1.41×10^{-2}	0.378
1.59×10^{-2}	0.361
2.20×10^{-2}	0.335
2.34×10^{-2}	0.332
3.71×10^{-2}	0.284
5.28×10^{-2}	0.262

[a] Measured at 35°C for a 10^{-2} M solution of **1a** in 0.066 M phosphate buffer (pH 6.0).

[b] Calculated (eq. 9) for an association constant, $K = 25\ \text{M}^{-1}$.

Table 2

$T_1(^2H)$ values measured for methyl-d_3 *N*-acetyl-β-D-glucosaminide (**1b**) in the presence of increasing amounts of lysozyme [a]

$C = [EI]/[I_0]$ [b]	T_1 (OMe) (s)
0.00	0.473
1.35×10^{-3}	0.464
3.56×10^{-3}	0.451
6.64×10^{-3}	0.430
1.08×10^{-2}	0.400
2.23×10^{-2}	0.363
2.84×10^{-2}	0.340
3.60×10^{-2}	0.328
4.48×10^{-2}	0.301
7.40×10^{-2}	0.259

[a] Measured at 35 °C for a 10^{-2} M solution of **1b** in 0.066 M phosphate buffer (pH 6.0).
[b] Calculated (eq. 9) for an association constant, $K = 35$ M^{-1}.

eq. 1. For the system under study, the value of τ_M has been determined [13] to be approx. 0.2 ms. Inspection of T_{1M} values in table 6 reveals that this contribution is certainly negligible for the *O*-methyl groups.

Increasing lysozyme concentrations cause considerable line broadening of the C2-^{2}H signal for both anomers, **1a′** and **1b′**, and this makes T_1

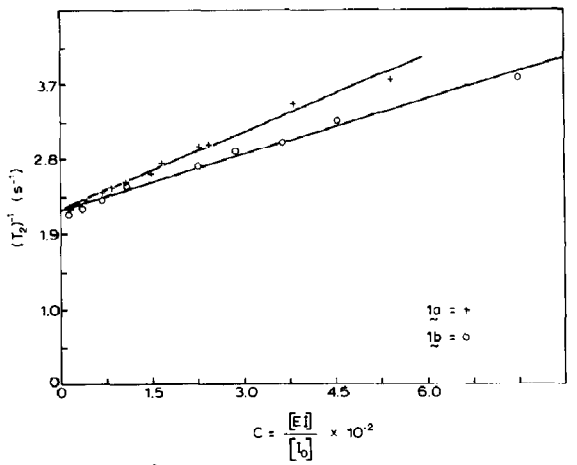

Fig. 1. Plots of ^{2}H spin-lattice relaxation rates for *O*-methyl-d_3 groups in Me α- (**1a**) and -β-GlcNAc (**1b**) as a function of the mole fraction bound to lysozyme ($C = [EI]/[I_0]$). The inhibitor concentration was 10^{-2} M in 0.066 M phosphate buffer (pH 6.0) at 35 °C. The correlation coefficients for the linear fits are 0.996 and 0.994 for **1a** and **1b**, respectively.

Table 3

^{2}H linewidths for methyl *N*-acetyl-α-D-glucosaminide-C2-d (**1a′**) in the presence of increasing amounts of lysozyme [a]

$C = [EI]/[I_0]$ [b]	$\Delta\nu_{1/2}$ [c] (Hz)
0.00	6.0
1.90×10^{-3}	7.1
3.65×10^{-3}	7.7
6.38×10^{-3}	9.6
1.18×10^{-2}	11.5
1.97×10^{-2}	10.4
2.28×10^{-2}	14.6
5.42×10^{-2}	20.8
6.50×10^{-2}	23.7

[a] Measured at 35 °C for a 1.09×10^{-2} M solution of **1a′** in 0.066 M phosphate buffer (pH 6.0).
[b] Calculated (eq. 9) for an association constant, $K = 25$ M^{-1}.
[c] $\Delta\nu_{1/2} = \Delta\nu_{1/2}(\text{obs}) - \Delta\nu_{1/2}(\text{HDO})$, where $\Delta\nu_{1/2}$ values have been obtained through spectrum deconvolution; see section 3.

measurements inaccurate in these cases. We have therefore determined T_2 values through linewidth measurements. Because of partial overlap with the HDO resonance, accurate linewidth values have been determined through computer deconvolution [14] of the HDO and C2-^{2}H resonances using Lorentzian lineshapes (fig. 3). To obtain T_2 values for the C2-^{2}H label, the linewidths have been corrected by $\Delta\nu_{1/2}$ values of the HDO-resonance. The pertinent experimental data are summarized

Table 4

^{2}H linewidths for methyl *N*-acetyl-β-D-glucosaminide-C2-d (**1b′**) in the presence of increasing amounts of lysozyme [a]

$C = [EI]/[I_0]$ [b]	$\Delta\nu_{1/2}$ [c] (Hz)
0.00	6.6
2.61×10^{-3}	7.4
5.23×10^{-3}	9.0
9.08×10^{-3}	10.3
1.21×10^{-2}	12.0
2.04×10^{-2}	13.5
2.57×10^{-2}	15.6
3.56×10^{-2}	18.7
4.26×10^{-2}	18.8
6.79×10^{-2}	23.3

[a] Measured at 35 °C for a 1.25×10^{-2} M solution of **1b′** in 0.066 M phosphate buffer (pH 6.0).
[b] Calculated (eq. 9) for an association constant, $K = 35$ M^{-1}.
[c] See footnote c to table 3.

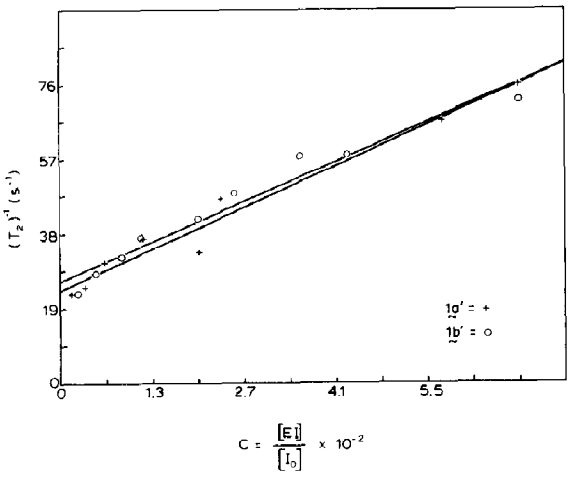

Fig. 2. Plots of ^{2}H spin-spin relaxation rates, $T_2^{-1} = [\Delta\nu_{1/2}(\text{obs}) - \Delta\nu_{1/2}(\text{HDO})]\pi$ vs complexed fraction ($C = [EI]/[I_0]$) for the C2-^{2}H resonances in Me α- (**1a'**) and -β-GlcNAc (**1b'**) for inhibitor concentrations of 1.09×10^{-2} M (**1a'**) and 1.25×10^{-2} M (**1b'**) in 0.066 M phosphate buffer (pH 6.0) at 35°C. The correlation coefficients for the best fit lines are 0.984 (**1a'**) and 0.987 (**1b'**).

in tables 3 and 4 and a linear fit is shown in fig. 2. It is apparent from table 6 that the exchange contribution, τ_M, is not negligible for the relaxation of the deuteron at position 2; a maximum of 15% can be estimated from the data cited above. This was taken into account when calculating τ_b values (table 6).

The ^{2}H label in position 2 reports on the overall motion of the sugar ring. In the enzyme-bound state the rotational correlation time for this label is approx. two orders of magnitude longer (table 6) than in the unbound environment (table 5) for both **1a'** and **1b'**. Rotational correlation times in the range of $2.8–10\times10^{-9}$ s have been reported [15–17] for lysozyme. Since the present measurements were performed at a higher temperature, it is reasonable to assume shorter values for further consideration. In this case the correlation times of the sugar ring for both **1a'** and **1b'** are very close to that of the enzyme indicating virtually complete immobilization upon binding. This result is in agreement with X-ray crystallographic evidence [2,18] and, more importantly, provides direct experimental confirmation, in the liquid state, of the assumption we made previously [4] with regard to inhibitor binding to lysozyme. It should be noted

Table 5

^{2}H and ^{13}C relaxation data for the free inhibitors, **1a**, **1a'** and **1b**, **1b'** [a]

	T_1, $T_2(^2H)$ [b] (s)	$T_1(^{13}C)$ [c] (s)	$\tau_f(^2H)$ [c] (s)	$\tau_f(^{13}C)$ [d] (s)
1a' C-2	0.053	1.00	4.4×10^{-11}	4.3×10^{-11}
1a OMe	0.453	2.44	5.1×10^{-12}	5.9×10^{-12}
1b' C-2	0.048	0.90	4.8×10^{-11}	4.7×10^{-11}
1b OMe	0.473	2.00	4.9×10^{-12}	7.1×10^{-12}

[a] For measurement conditions see footnotes to tables 1–4.

[b] $T_1(^2H)$ values for *O*-methyl-d_3 and $T_2(^2H)$ values for C2-^{2}H as determined from linear fits of eq. 2 to the data in tables 3 and 4. The correlation coefficients for the linear fits varied between 0.992 and 0.996.

[c] Calculated from $T_{1,2}^{-1} = 3/8[(e^2qQ/\hbar)^2\tau_f]$ for a quadrupolar coupling constant e^2qQ/h equal to 170 kHz.

[d] Calculated from $T_1^{-1} = N\frac{\hbar^2\gamma_C^2\gamma_H^2}{r_{CH}^6}\cdot\tau_f$ for a C–H bond length of 1.08 Å.

[e] Measured on non-deuterated samples.

Table 6

^{2}H relaxation data for the inhibitors, **1a**, **1a'** and **1b**, **1b'** in the lysozyme-bound state [a]

	T_{1M}, T_{2M} [b] (s)	T_{1b}, T_{2b} [b,c] (s)	b [d] (s)	T_{1b}^{-1}, T_{2b}^{-1} (s^{-1})
1a' C-2	1.2×10^{-3}	1.0×10^{-3}	3.0×10^{-9}	1000
1a OMe	3.08×10^{-2}	3.06×10^{-2}	7.6×10^{-11}	32.7
1b' C-2	1.2×10^{-3}	1.0×10^{-3}	3.0×10^{-9}	1000
1b OMe	4.24×10^{-2}	4.22×10^{-2}	5.5×10^{-11}	23.7

[a,b] See respective footnotes to table 5; the correlation coefficients for the linear fits were 0.984–0.987.

[c] $T_{ib} = T_{iM} - \tau_M$ $i = 1, 2$; see eq. 2; $\tau_M = k_4^{-1} = 2\times10^{-4}$ s [4].

[d] Calculated from eqs 4–6.

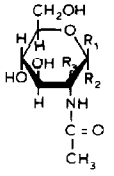

	R_1	R_2	R_3
1a	H	OC^2H_3	H
1a'	H	OCH_3	^2H
1b	OC^2H_3	H	H
1b'	OCH_3	H	^2H

Scheme 1.

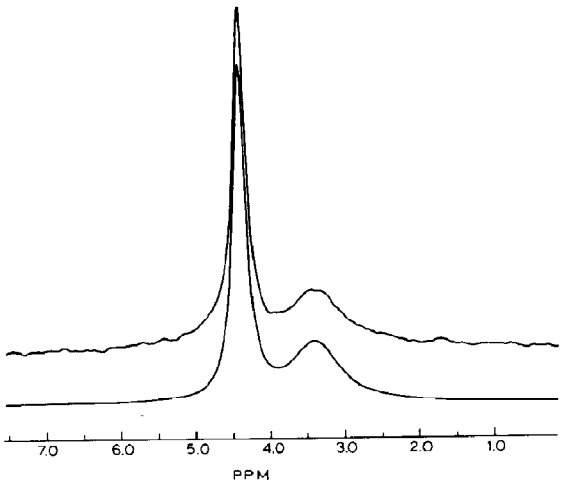

Fig. 3. Example showing the spectrum deconvolution for determination of the linewidth for the C2-^{2}H resonance of Me β-NAcGlc (**1b**) for a bound mole fraction ($C = [EI]/[I_0]$) of 3.56×10^{-2}. (Top) Experimental, (bottom) calculated [14]. Other experimental conditions are listed in fig. 2.

that the two anomers, **1a'** and **1b'**, display identical behaviour as far as the sugar ring motion upon binding is concerned.

As for the glycosidic methyl groups, inspection of table 6 indicates that they retain a considerable degree of internal motion in the bound state. Since the effective correlation times for the methyl groups [τ_b(OMe)] in both anomers (**1a** and **1b**) are 1–1.5 orders of magnitude shorter than those for the sugar ring, it is evident that fast internal rotation around one axis prevails for these groups (vide infra) in the EI complexes. Eq. 8 can be used to estimate the contribution of τ_r, provided τ_c, the correlation time for the overall reorientation, is accessible independently. In the present case, τ_c can be taken to be equal to the rotational correlation time measured for the C2-^{2}H label in the bound state [τ_b(C2-^{2}H], table 6). At the magnetic field strength used in the present study (4.7 T), the correlation time for internal rotation (τ_r) calculated from eq. 8 is:

$$\tau_r = \frac{(T_{1b})^{-1} - (T_{1calc})^{-1}}{1.4 \times 10^{12}} \qquad (10)$$

where the quantity of $9.5 \times 10^9 \cdot f_1(\tau_c)$ in eq. 8 has been denoted as $(T_{1calc})^{-1}$. Taking τ_c equal to τ_b(C2-^{2}H) (table 6) as mentioned above, we obtain approx. 71 s^{-1} for $(T_{1calc})^{-1}$. This is reasonably close to the $(T_{1b})^{-1}$ values for the *O*-methyl deuterons (table 6) if allowance is made for experimental errors and approximation [10] in the model used (eq. 8). Since eq. 10 predicts, for the present case, fast internal rotation [$\tau_r \sim 0.1 \times \tau_b$(C2-^{2}H)] as long as the numerator is less than approx. 100, the present experimental data are fully compatible with the assumption that fast internal rotation of the *O*-methyl groups is retained in both inhibitor molecules (**1a** and **1b**) in the enzyme-bound state. A small but consistent decrease in relaxation rate for the *O*-methyl deuterons is observed in the E-**1b** complex with respect to E-**1a** (table 6). At present, it is difficult to tell whether this difference is significant enough for a comparison to be made between the solution structures of these complexes. Nevertheless, it should be noted, that a similar difference for *N*-acetylmethyl rotations in E-**1a** and E-**1b** has previously been observed [4]. It is known that the binding mode of αGlcNac to lysozyme is different from that of βGlcNac in the solid state [2,18,19].

5. Conclusion

In summary the molecular dynamics of methyl *N*-acetyl α- and β-D-glucosaminide inhibitors bound to hen egg white lysozyme has been characterized through ^{2}H relaxation measurement using multiply ^{2}H-labeled compounds. Analysis of T_1 and T_2 data for the ^{2}H labels at position 2 of the tetrahydropyrane ring and in the glycosidic methyl group has revealed that, while the sugar ring is tightly bound to the enzyme in both complexes, E-**1a** and E-**1b**, the *O*-methyl groups retain fast internal rotation around one axis in both cases. Whereas the rotational correlation times for the ring motion (as measured by the C2-^{2}H label) are essentially identical in the two complexes, E-**1a** and E-**1b**, a slight but consistent difference in the relaxation rates of the glycosidic *O*-methyl groups may indicate different solution structures for these enzyme-inhibitor complexes.

Acknowledgement

This study has been supported by a grant, OTKA 274/86, from the Hungarian Academy of Sciences.

References

1 K. Hamaguchi and K. Hayashi, Molecular basis of enzyme function — Lysozyme (Kodansha, Tokyo, 1978).
2 C.C.F. Blake, L.N. Johnson, G.A. Mair, A.C.T. North, D.C. Phillips and V.R. Sarma, Proc. Roy. Soc. Lond. 167B (1967) 378.
3 C.A. Vernon, Proc. Roy. Soc. Lond. 167B (1967) 389.
4 L. Szilágyi, J. Harangi and L. Radics, Biophys. Chem. 6 (1977) 201.
5 K.J. Neurohr, N. Lacelle, H.H. Mantsch and I.C.P. Smith, Biophys. J. 32 (1980) 931.
6 T.J. Swift and R. Connick, J. Chem. Phys. 37 (1962) 307.
7 Z. Luz and S. Meiboom, J. Chem. Phys. 40 (1964) 2686.
8 A. Abragam, The principles of nuclear magnetism (Clarendon, Oxford, 1961) 313.
9 D. Wallach, J. Chem. Phys. 47 (1967) 5258.
10 J. Andrasko and S. Forsén, Chem. Scr. 6 (1974) 163.
11 C. Brévard, J.-P. Kintzinger and J.-M. Lehn, Tetrahedron 28 (1972) 2429.
12 R.U. Lemieux, S. Koto and C. Voisin. Am. Chem. Soc., Symp. Ser. 87 (1979) ch. 2.
13 B.D. Sykes, Biochemistry 8 (1969) 1110.
14 P. Barron, LINESIM program, ABACUS Library no. ABAO51, Spectrospin AG, Fallanden/Zürich (1989).
15 S.B. Dubin, N.A. Clark and G.B. Benedek, J. Chem. Phys. 54 (1971) 5158.
16 I.D. Campbell, C.M. Dobson and R.J.P. Williams, J. Chem. Soc. Chem. Commun. (1974) 888.
17 R.A. Dwek, in: NMR in biochemistry (Clarendon, Oxford, 1973) p. 303.
18 P.J. Perkins, L.N. Johnson, P.A. Machin and D.C. Phillips, Biochem. J. 173 (1978) 607.
19 C.R. Beddell, J. Moult and D.C. Phillips, Molecular properties of drug receptors (Churchill, London, 1970).
20 F. Zilliken, C.S. Rose, G.A. Braun and P. György, Arch. Biochem. Biophys. 54 (1955) 392.
21 L. Szilágyi, P. Herczegh and Gy. Bujtás, Z. Naturforsch. 32b (1977) 296.
22 R.C. Davies, A. Neuberger and B.M. Wilson, Biochim. Biophys. Acta 178 (1969) 294.
23 G.H. Weiss and J.A. Ferretti, Prog. NMR Spectrosc. 20 (1988) 317.
24 A.J. Shaka and R. Freeman, J. Magn. Reson. 55 (1983) 487.
25 D.R. Bundle, H.J. Jennings and I.C.P. Smith, Can. J. Chem. 51 (1973) 3812.